Facile Nonsurfactant Route to Silica-based Bimodal Xerogels with Micro/Mesopores

Dongjiang Yang,[†,††] Yao Xu,[†] Shangru Zhai,[†,††] Junlin Zheng,[†,††] Junping Li,[†,††] Dong Wu,[†] and Yuhan Sun*[†]
[†]*State Key Laboratory of Coal Conversion, Institute of Coal Chemistry, Chinese Academy of Sciences, Taiyuan 030001, P. R. China*
[††]*Graduate School of the Chinese Academy of Sciences, Beijing 100039, P. R. China*

(Received May 11, 2005; CL-050627)

A simple and nonsurfactant synthesis pathway has been developed to prepare silica-based bimodal micro/mesoporous hybrids using mixed polymethylhydrosiloxane and tetraethyl orthosilicate as silica sources.

Since the discovery of mesoporous silica-based materials by researchers at Mobil Oil Company[1,2] and scientists of Japan[3] in the early 1990s, remarkable new opportunities have been created to prepare micro/mesoporous bimodal composites because of their potential applications in catalysis, adsorption, and separation processes. With the successful synthesis of zeolite faujasite (FAU) and MCM-41, Kloetstra et al.[4] have obtained a composite of FAU and MCM-41 with the overgrowth of a thin layer of MCM-41 on FAU, and good results were achieved using this composite for vacuum gas oil cracking. Karlsson et al.[5] prepared composite materials by simultaneous synthesis of MFI/MCM-41 phase using two-template approach at optimized template concentrations and reaction temperatures. Furthermore, Li et al.[6] prepared a MCM-41/β composite by two-step crystallization, which has dual acidity and pore structure. Recently, we have successfully synthesized methyl-modified mesoporous materials with dual porosity using nonionic surfactant.[7] Although significant progress has been made on the synthesis of micro/mesoporous materials, to the best of our knowledge, there are no reports on bimodal materials with micro/mesopores using nonsurfactant route.

Here, we report the novel synthesis of organic–inorganic micro/mesoporous xerogels using mixed tetraethyl orthosilicate (TEOS) and polymethylhydrosiloxane (PMHS) which is mainly employed as reducing agent for halogens, ketones, ethers, imines, and phosphine oxides[8,9] as silica sources via sol–gel route, without additional introduction of any surfactants.

In a typical synthesis, 2.35 mL (2.338 g) and 4.70 mL (4.676 g) of PMHS were dripped into two flasks containing 70 mL ethanol, respectively. The formed liquids were further stirred for 48 h at room temperature to allow PMHS to react with a part of C_2H_5OH and release hydrogen in the presence of NaOH as catalyst. Then 5 mL (4.676 g) of TEOS and determined deionized water were introduced to the two systems with vigorous stirring for 3 h, respectively. The formed sols were statically aged for 4–5 d and finally turned into gels. The obtained gels were heated in a 333 K vacuum oven to remove the C_2H_5OH, and corresponding to the PMHS/TEOS mass ratio of 1:1 and 1:2, they were designated as sample M1 and M2, respectively. The newly obtained xerogels were characterized by X-ray diffraction (XRD), nitrogen adsorption, Fourier-transform infrared spectroscopy (FTIR), transmission electron microscopy (TEM), and scanning electron microscopy (SEM) without any solvent extraction and calcination.

Table 1. The surface area data and pore parameters of the obtained xerogels measured by different adsorption models

Sample	PMHS:TEOS (mass ratio)	BET surface area /$m^2\ g^{-1}$	Micropore[a] surface area /$m^2\ g^{-1}$	Limiting[a] micropore volume /$cm^3\ g^{-1}$
M1	1:1	490	282	0.124
M2	1:2	600	306	0.137

[a]Obtained by Dubinin–Astakhov model.

Table 1 is a compilation of the surface area and pore volume of different xerogels. Obviously, a high BET surface area (490 and 600 $m^2\ g^{-1}$) indicate the formation of porous structures.[10] On the other hand, the micropore surface area and limiting micropore volume measured by Dubinin–Astakhov model[11] show the existence of microphase in M1 and M2. The nitrogen adsorption isotherms for the xerogels are shown in Figure 1. Clearly, they all exhibit a resolved type IV isotherm with a steep desorption branch and a type H2 (type E in de Boer classification) hysteresis loop.[12] The desorption inflection point is very smooth and the desorption hysteresis loop at low relative pressure P/P_0 values is not closed, strongly indicating the nitrogen filling in micropores.[13,14] Furthermore, according to the observation by the pore size distribution plots obtained by density functional theory[15] (DFT) (inset in Figure 1), some supermicropores with radius less than 2 nm and mesopores around at 3 nm are present in the samples, showing bimodal pore

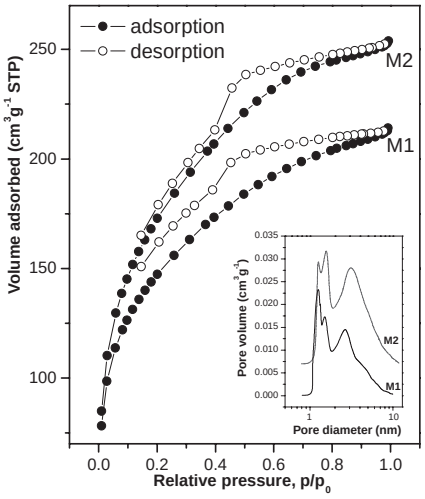

Figure 1. Nitrogen adsorption–desorption isotherms of the synthesized bimodal porous xerogels. Inset: DFT pore size distributions. (The plot M2 was shifted by 0.007 cm^3/g along with *y* axis for clarity).

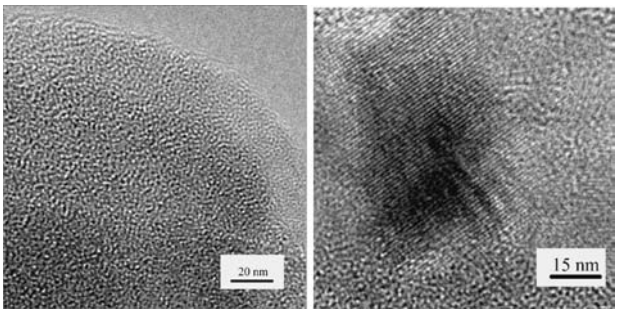

Figure 2. TEM images of the bimodal xerogel M2: region of wormhole pore structure (left) and small part of ordered-like pore arrays (right).

size distribution.

To further elucidate that the samples are porous materials, detailed pore structure was studied by HRTEM technique, and Figure 2 shows two repersentative TEM images of the xerogel M2 taken in different regions. Clearly, Figure 2 (left) depicts a direct image of the 3D wormhole-like pore frameworks (≈3 nm), which is very similar to those pore arrays of MSU-X type mesosilicas without long-range ordering.[16] Figure 2 (right) shows a region with layers of dark stripes which allow one to determine the supermicropore size (≈1.5 nm), and this image is consistent with a 2D cylindrical sturcuture viewed from the edge of the cylinders similar to those of 2D hexagonal MCM-41 or SBA-15.[17] At the same time, we can also clearly observe that other parts in this image appear to be disordered as shown in Figure 2 (left). They are in good agreement with the results obtained by nitrogem adsorption measurement.

It should be noted that, although there is a small part of ordered-like pore arrangement present in the xerogels, in fact, the material is almost completely composed of disordered pore arrays viewed through the TEM image. Although small oriented domains are observed in the TEM images, the presence of bimodal characteristics and large amount of $-CH_3$ organic group in the xerogel may lead to no observable peak in the low-angle region (not shown here) typical of mesoporous materials.[18]

Figure 3 shows the FTIR spectrum of sample M2. Noticeably, the peak at 2160 cm^{-1} relative to the stretching vibration of Si–H[19] disappears, indicating PMHS has reacted fully with C_2H_5OH. The band at 3330 cm^{-1} is mainly assigned to the –OH stretching vibration, and the peak at 1620 cm^{-1} is ascribed to a trace amount of H_2O in the KBr tablet. The peak at 2980 cm^{-1} could be attributed to the symmetric and antisymmetric C–H stretching vibration of $-CH_3$. Moreover, the sharp peaks at 1275 cm^{-1} and 775 cm^{-1} are due to the stretching vibration and bending vibration of Si–CH_3, respectively. The band at 1055 cm^{-1} was assigned to the stretching vibration of Si–O–Si, and the peak at 455 cm^{-1} was associated with the rocking vibration of Si–O–Si.

In summary, the silica-based bimodal micro/mesoporous xerogels could be facilely prepared using TEOS and PMHS via the present novel nonsurfactant pathway. Although the detailed formation mechanism is not fully determined at the present time, the current method can be used to prepare methyl-modified functional materials.

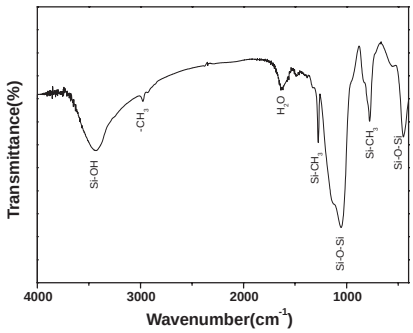

Figure 3. The FTIR spectrum of sample M2.

Financial support from the National Key Native Science Foundation (20133040) is gratefully acknowledged.

References

1 C. T. Kresge, M. E. Leonowicz, W. J. Roth, J. C. Vartuli, and J. S. Beck, *Nature*, **359**, 710 (1992).
2 J. S. Beck, J. C. Vartuli, W. J. Roth, M. E. Leonowicz, C. T. Kresge, S. B. Mccullen, J. B. Higgins, and J. L. Schlenker, *J. Am. Chem. Soc.*, **104**, 10834 (1992).
3 T. Yanagisawa, T. Shimizu, K. Kuroda, and C. Kato, *Bull. Chem. Soc. Jpn.*, **63**, 988 (1990).
4 K. R. Kloetstra, H. W. Zandbergen, J. C. Jansen, and H. van Bekkum, *Microporous Mater.*, **6**, 287 (1996).
5 A. Karlsson, M. Stocker, and R. Schmidt, *Microporous Mesoporous Mater.*, **27**, 181 (1999).
6 L. Huang, W. Guo, P. Deng, Z. Xue, and Q. Li, *J. Phys. Chem. B*, **104**, 2817 (2000).
7 Y. Zhang, J. M. Kim, D. Wu, Y. H. Sun, D. Y. Zhao, and S. Y. Peng, *J. Non-Cryst. Solids*, **251**, 777 (2005).
8 N. J. Lawrence and S. M. Bushell, *Tetrahedron Lett.*, **41**, 4507 (2000).
9 V. Bette, A. Mortreux, C. W. Lehmann, and J. F. Carpentier, *Chem. Commun.*, **2003**, 332.
10 N. K. Raman, M. T. Anderson, and C. J. Brinker, *Chem. Mater.*, **8**, 1682 (1996).
11 M. M. Dubinin, *Carbon*, **25**, 593 (1987).
12 K. S. W. Sing, D. H. Everett, R. A. W. Haul, L. Moscou, R. A. Pierotti, J. Rouquerol, and T. Siemieniewska, *Pure Appl. Chem.*, **57**, 603 (1985).
13 P. Messina, M. A. Norini, and P. C. Schulz, *Colloid Polym. Sci.*, **282**, 1063 (2004).
14 M. Kruk, M. Jaroniec, and A. Sayari, *Adsorption*, **6**, 47 (2000).
15 M. Kruk, M. Jaroniec, and Y. Berezniski, *J. Colloid Interface Sci.*, **182**, 282 (1996).
16 W. Zhu, Y. Han, and L. An, *Microporous Mesoporous Mater.*, **71**, 137 (2004).
17 Y. Sakamoto, M. Kaneda, O. Terasaki, D. Y. Zhao, J. M. Kim, G. Stucky, H. J. Shin, and R. Ryoo, *Nature*, **408**, 449 (2000).
18 X. Wang, W. Li, G. Zhu, S. Qiu, D. Zhao, and B. Zhong, *Microporous Mesoporous Mater.*, **71**, 87 (2004).
19 B. Y. Zhang, S. M. Guo, and B. Shao, *J. Appl. Polym. Sci.*, **68**, 1555 (1998).

Published on the web (Advance View) July 16, 2005; DOI 10.1246/cl.2005.1138